

UDC 539.2

**QUANTUM DYNAMICAL STUDY OF HEAVY-LIGHT-HEAVY REACTIONS:
APPLICATION TO THE (Cl + CH₄ → HCl + CH₃) REACTION****A.H. Moussa¹, M. Shalaby¹, H. Talaat¹, S. El-Wallid Sedik², M.T. El-Din Kamal²**¹*Physics Department, Faculty of Science, Ain Shams University, Cairo, Egypt*²*Theoretical Physics Department, National Research Center, Dokki, Giza, Egypt*

E-mail: esedik@gmail.com

*Received December, 2, 2013**Revised February, 19, 2014*

A time dependent quantum-mechanical QM study is performed on the Cl + CH₄ → HCl + CH₃ reaction, using a pseudotriatomic *ab initio* based surface. Probabilities present some clear peaks versus *t*, which we assign to transition state resonances where the light H atom oscillates between heavy Cl and CH₃ groups. For ground-state reactants, the reactivity is of quantum origin. The reaction occurs through an abstraction mechanism, following both direct and an indirect mechanisms. The calculations show the participation of a short-lived collision complex in the microscopic reaction mechanism. This theoretical result and other oscillating properties found here could, however, be related to the existence of resonance for the production of HCl, as suggested by experimentalists.

DOI: 10.15372/JSC20150710

Keywords: reaction dynamics, potential surface, normal modes, Cl + CH₄ → HCl + CH₃ reaction.**INTRODUCTION**

The gas phase chemical reactions associated with the ozone depletion in the stratosphere have been the subject of different experimental and theoretical studies in recent time. The chlorine radical has been discovered to be an active catalyzer of some cycles that may efficiently cause ozone destruction. The reactions that can play role for chlorine are therefore highly attractive candidates for experimental and theoretical studies. This is the case of Cl reactions with hydrocarbons, which transform the chlorine radical into the less active HCl molecule [1]. The most abundant hydrocarbon present in the atmosphere is methane and its reaction with chlorine is the first source of deactivation of the Cl radical in the stratosphere. Hence, the wealth of experimental contributions on this reaction regarding the reaction dynamics, the experiments of Zare *et al.* [2—10] furnished a wide variety of results dealing with a broad spectrum of dynamic properties of the titled reaction with methane in its ground vibrational state. Those investigations are particularly important, since the experiments went beyond the measurement of vibrational distributions of the HCl molecule formed in the reactive process. One of the most relevant conclusions of that work was that a low amount of available energy was released as the internal energy of the CH₃ radical. The present collision follows a heavy-light-heavy HLH kinematics, where the light atom can be temporarily trapped and oscillating between the two heavy atoms. This can give resonances [11], i.e., quasi-bound quantum states, collision complexes leading quickly to products. Therefore, this HLH reactive system [12] may show significant quantum effects, such as oscillations in reaction probabilities and tunneling dynamics.

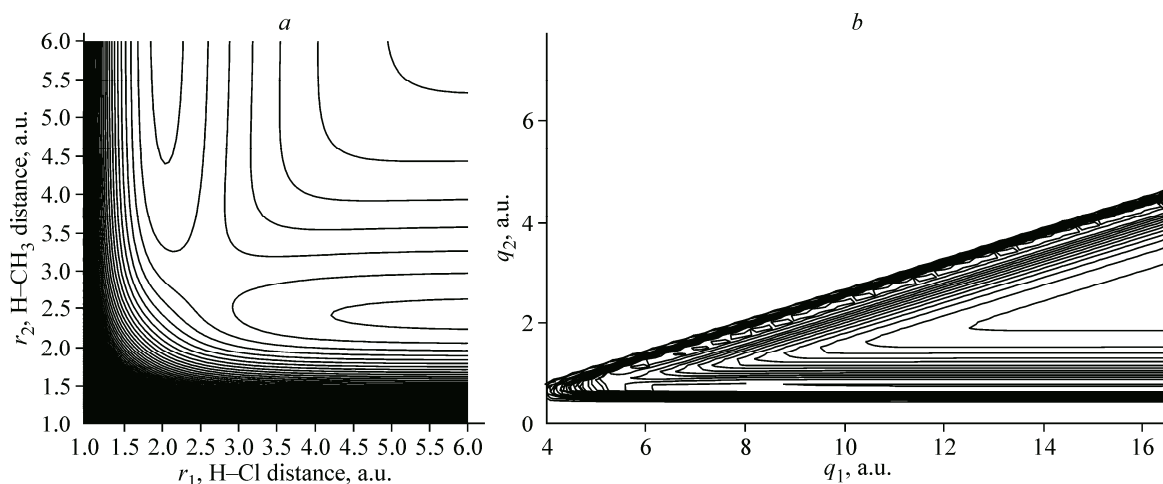


Fig. 1. 2D view of the potential energy surface for the $\text{Cl} + \text{CH}_4 \rightarrow \text{HCl} + \text{CH}_3$ reaction. The $\text{Cl}-\text{H}-\text{CH}_3$ angle is linear. The lowest potential curve is 2.306 kcal/mol above the minimum at large separations of the reactants. The interval between curves is 4.612 kcal/mol

THEORETICAL

Potential energy surface. The calculations [13] were carried out using unrestricted second-order Møller-Plesset perturbation theory including excitations from inner shell electrons and using a large polarized basis set supplemented with diffuse functions on all atoms [UMP2(full)/6-311++G(2d,2p)]. Fig. 1 shows the 2D view of the potential energy surface (PES) for the $\text{Cl} + \text{CH}_4 \rightarrow \text{HCl} + \text{CH}_3$ reaction. The $\text{Cl}-\text{H}-\text{CH}_3$ angle is linear. The lowest potential curve is 2.306 kcal/mol above the minimum at large separations of the reactants. The interval between curves is 4.612 kcal/mol.

Normal modes are important to monitor the geometry of the molecule and in an ion system, especially in explaining the atmospheric (ozone) reactions.

Figs. 2—5 show the variation of the generalized normal modes (vibrational frequencies) on the potential surface for the $\text{C} + \text{CH}_4$ reaction. In the negative limit of s , the frequencies are associated with the reactants, while in the positive limit of s , the frequencies are associated with the products.

Theory. We have calculated quantum reaction probabilities via the time dependent wave packet method, defining an initial wave packet. The time-dependent Schrödinger equation in which the quantum dynamical behavior of our model system is contained can be expressed shortly as

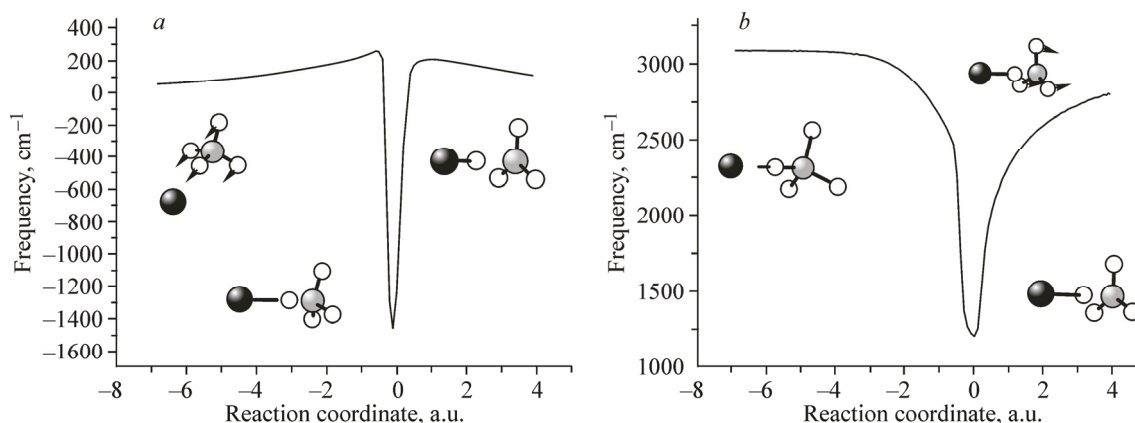


Fig. 2. Translational frequency determined along IRP by the method of Miller et al. The translational frequency having negative values corresponds to imaginary frequencies (a). Harmonic vibrational frequencies belonging to the irreducible representation $A_1(\omega_1^{A_1})$ which gives the HCl vibration (b)

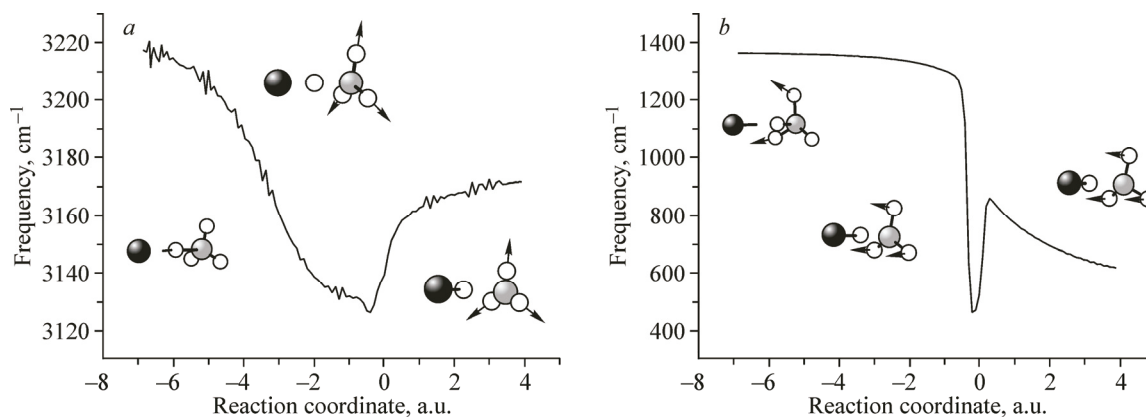


Fig. 3. Harmonic vibrational frequencies belonging to the irreducible representation $A1$ (ω_2^{A1}) (a) and $A1$ (ω_3^{A1}) (b)

$$i\hbar \frac{\partial \Psi}{\partial t} = \hat{H} \Psi(r_1, r_2, t), \quad (1)$$

$$H = -\frac{\hbar^2}{2} \left[\left(\frac{1}{m_1} + \frac{1}{m_2} \right) \frac{\partial^2}{\partial r_1^2} + \left(\frac{1}{m_2} + \frac{1}{m_3} \right) \frac{\partial^2}{\partial r_2^2} - \frac{2}{m_2} \frac{\partial^2}{\partial r_1 \partial r_2} \right] + V(r_1, r_2).$$

By introducing the skewed coordinates q_1, q_2 it becomes

$$H = -\frac{\hbar^2}{2\mu} \left[\frac{\partial^2}{\partial q_1^2} + \frac{\partial^2}{\partial q_2^2} \right] + V(q_1, q_2),$$

where

$$\mu = \left[\frac{m_1 m_2 m_3}{m_1 + m_2 + m_3} \right]^{1/2}$$

can be formally integrated to give

$$\Psi(r_1, r_2, \Delta t) = U(\Delta t) \Psi(r_1, r_2, 0), \quad (2)$$

where $U(\Delta t) = \exp[-(i\Delta t/\hbar)H]$ is the time evolution operator. In order to advance the wave function through n time steps, we repeatedly apply $U(\Delta t)$ starting with the initial wave function using high or der finite difference algorithms [13]. After n steps, we have

$$\Psi(r_1, r_2, n\Delta t) = U^n(\Delta t) \Psi(r_1, r_2, 0). \quad (3)$$

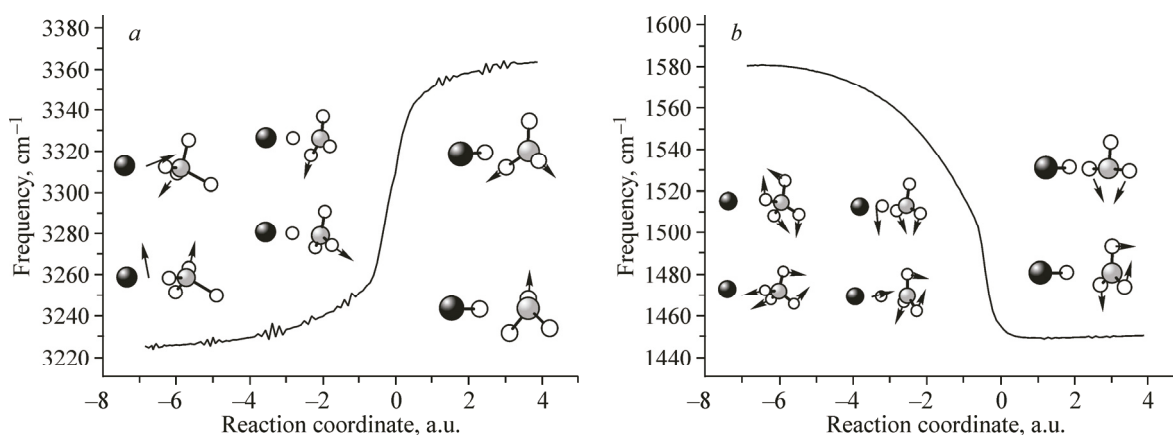


Fig. 4. Harmonic vibrational frequencies belonging to the irreducible representation E (ω_1^E) (a) and E (ω_2^E) (b)

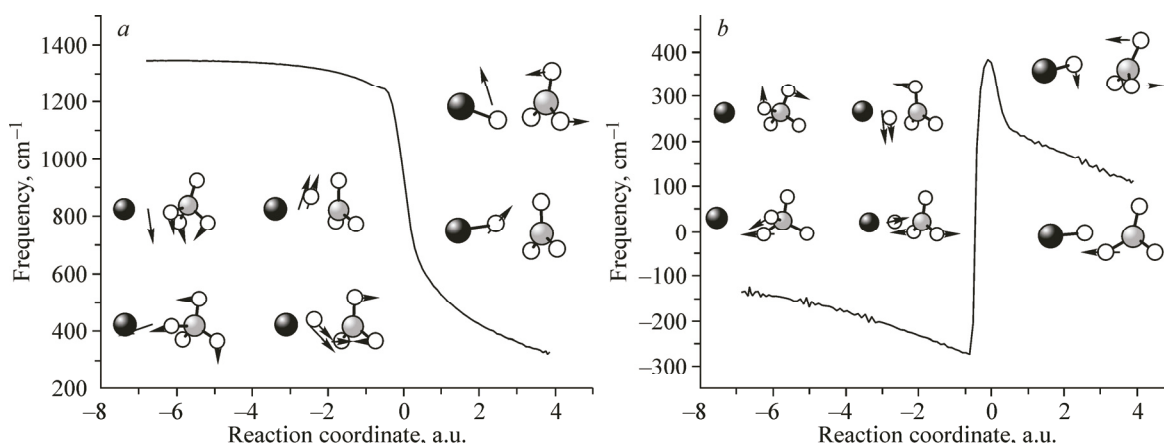


Fig. 5. Harmonic vibrational frequencies belonging to the irreducible representation $E(\omega_3^E)$ (a) and $E(\omega_4^E)$ (b)

The wave function is specified at the time $t = 0$ and propagated to later times. The wave packet is needed to represent the initial state of the colliding system. Far from the interaction region of the PES, the initial wave packet is the product of a translational function for the relative motion times and the vibrational wave function for the BC molecule

$$\Psi(r_1, r_2, 0) = \psi_{tr}(R_A)\chi_v(r). \quad (4)$$

Here, R_A is the distance from atom A to the center of mass of BC. $\chi_v(r_1)$ is the v -th vibrational state of the diatomic reactant BC. The translational probability amplitude $\psi(R_A)$ is chosen to be a Gaussian wave packet parameterized by P_A^0 (the momentum conjugate to R_A), representing an impending collision with variable initial translational energy

$$\psi(R_A) = (2\pi\delta^2)^{-1/4} \exp[-(R_A - R_A^0)^2 / 4\delta^2] \exp[-ik_0 R_A], \quad (5)$$

where δ is the width parameter. The second exponential is the driving term which gives the wave packet an initial momentum toward the interaction region with the momentum $\hbar k_0$. The average kinetic energy of this translational packet is $\hbar^2(k_0^2 + 1/4\delta^2) / 2\mu$, where $\hbar^2 k_0^2 / 2\mu$ is the flow kinetic energy from the driving term and the remaining contribution is the shape of the wave packet as it propagates toward the interaction region. We have used Gaussian function (5) for the translational function in the initial wave packet in all our calculations.

For the vibrational wave function of the molecule which appears in equation (4) of the initial packet, we used the ground state Morse wave function

$$\chi(r) = N \exp\{-(b+1)/2 \exp[-\alpha(r-r_0)]\} \times \{(b+1) \exp[-\alpha(r-r_0)]\}^{b/2}, \quad (6)$$

where $b = (8\mu D)^{1/2} / \alpha \hbar - 1$. N is a normalizing factor, μ is the reduced mass of the molecule, and D , α , r_0 are the three Morse parameters.

For all the $\text{Cl} + \text{CH}_4 \rightarrow \text{HCl} + \text{CH}_3$ calculations the time interval is $\Delta t = 0.025 \text{ fs} = 0.025 \times 10^{-15} \text{ s}$, and mesh spacings are $\Delta q_1 = \Delta q_2 = 0.05 \text{ a.u.}$ (the mesh normally contains $\sim 10^6$ points). The center of the initial wave packet is placed at $q_1^0 = 8.5 \text{ a.u.}$ in the reactant region. For the width parameter δ in the Gaussian function (equation 5) we applied the value of 0.25 a.u. All calculations are carried out for reactant molecules in their ground vibrational states for collinear configurations of the three interacting species and for one translational energy value of the initial Gaussian wave packet, namely, 1.5 eV .

DISCUSSION AND CONCLUSIONS

CH_4 is treated as a pseudo-diatom QH (Q is a quasi-atom with the mass of CH_3) and the scattering calculations were restricted to collinear geometries with a linear transition state, which suggests that collinear geometries may dominate the reaction. The potential gives a vibrationally adiabatic ground

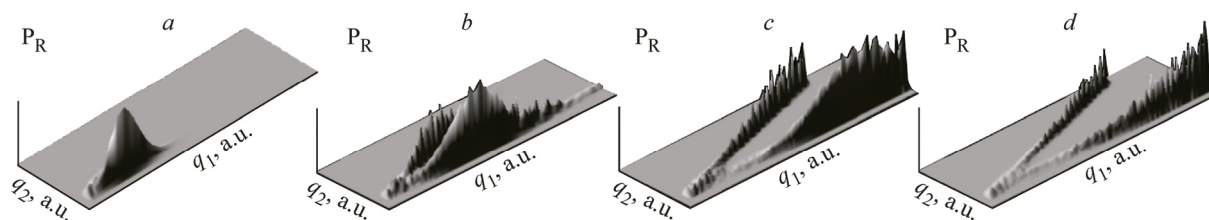
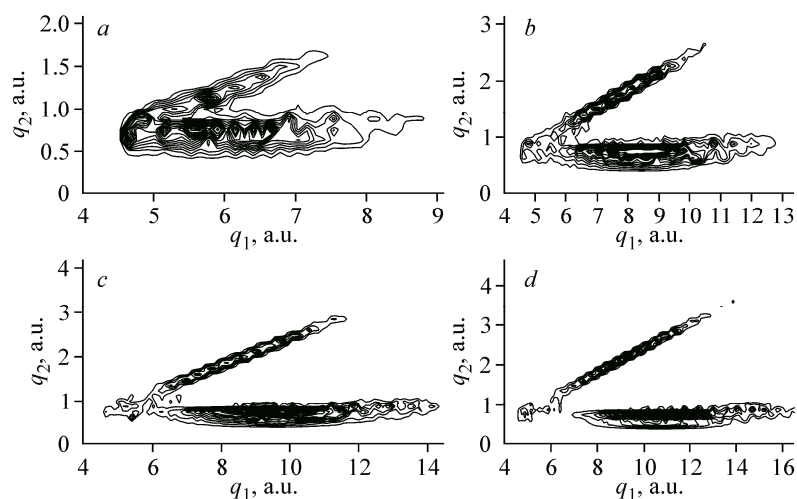


Fig. 6. "Snapshots" of the reaction probability for the collinear $\text{Cl} + \text{CH}_4 \rightarrow \text{HCl} + \text{CH}_3$ reaction on the PES for the case $v = 0$, $E_{\text{trans}} = 1.5$ eV. (One time step $\Delta t = 0.025$ fs)

Fig. 7. Contour plot of the reaction probability for the collinear $\text{Cl} + \text{CH}_4 \rightarrow \text{HCl} + \text{CH}_3$ reaction on the PES for the case $v = 0$, $E_{\text{trans}} = 1.5$ eV. (One time step $\Delta t = 0.025$ fs)



state barrier height of 3.5 kcal/mol. Bearing in mind the simplifications made in treating the $\text{Cl} + \text{CH}_4$ reaction, we have obtained some encouraging results.

The present study reports the results of the quantum mechanical wave packet approach for $\text{Cl} + \text{CH}_4 \rightarrow \text{HCl} + \text{CH}_3$ (PES). We visualize the wave packet propagation at fixed times in order to gain an insight into the nature of the reaction process. The initial Gaussian wave packet has its center placed at $q_1 = 8.5$ a.u. After 5000 time steps the center of the wave is found at $q_1 = 3.0$ a.u., as shown in Fig. 6, *a*. The wave packet has also clearly broadened. In Fig. 6, *b* (time step 7000), the wave packet is just entering the interaction region. At time step 7800 (Fig. 6, *c*) there are drastic alterations in the form of the wave packet, which shows multiple interference maxima. The largest maxima are on the left. Fig. 6, *a*, *b*, *c*, *d* shows such snapshots and Fig. 7, *a*, *b*, *c*, *d* is the contour plot. The region being viewed contains the reactant, the interaction, and the product regions.

At time steps $8000\Delta t$, $9000\Delta t$ Fig. 6, *c*, *d* shows the packet spreading and climbing the PES wall. It also shows the production of ripple maxima throughout the part of the wave-packet that reflects back into the reactant region.

At time steps 8500, 9000 Fig. 7, *a*, *b* shows the wave packet with multiple interference maxima. The largest maxima are on the left. At time steps $13000\Delta t$, $15000\Delta t$ Fig. 7, *c*, *d* shows the production of ripple maxima throughout the part of the wave-packet that reflects back into the reactant region.

The time threshold of the reaction for the calculations with the PES ranges from 5000 to 7000 time steps, the higher the collision energy is, the lower the

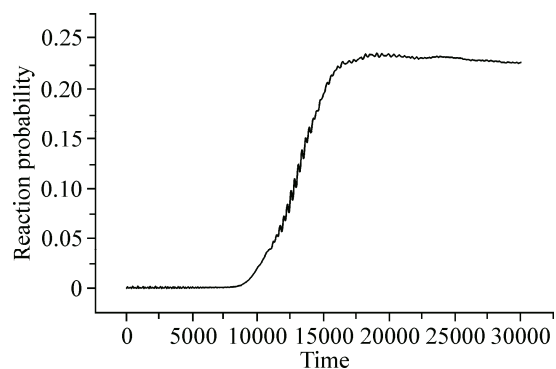


Fig. 8. Plot of the reaction probability versus time for the collinear $\text{Cl} + \text{CH}_4 \rightarrow \text{HCl} + \text{CH}_3$ reaction on the PES for the case $v = 0$, $E_{\text{trans}} = 1.5$ eV. (One time step $\Delta t = 0.025$ fs)

time threshold. The reaction probability increases smoothly in the time step range 5000—7800. Thereafter, it increases slowly until about 15000 time steps, where it becomes nearly constant. For the collision energy $E = 1.5$ eV the reaction probability is 0.23 (Fig. 8).

Probability shows some peaks versus t , which we assign to resonances of the transition state where the light H atom oscillates between heavy Cl and CH_3 groups. The calculations show the participation of a short-lived collision complex in the microscopic reaction mechanism. This theoretical result and other oscillating properties found here could, however, be related to the existence of resonance for the production of HCl as confirmed by theory [14, 15] and experiment [16—18].

REFERENCES

1. *Warneck P.* Chemistry of the Natural Atmosphere. – San Diego: Academic, 2000.
2. *Simpson W.R., Orr-Ewing A.J., Zare R.N.* // Chem. Phys. Lett. – 1993. – **212**. – P. 163.
3. *Simpson W.R., Rakitzis T.P., Kandel S.A., Orr-Ewing A.J., Zare R.N.* // J. Chem. Phys. – 1995. – **103**. – P. 7299.
4. *Simpson W.R., Rakitzis T.P., Kandel S.A., Orr-Ewing A.J., Zare R.N.* // J. Chem. Phys. – 1995. – **103**. – P. 7313.
5. *Simpson W.R., Rakitzis T.P., Kandel S.A., Lev-On T., Zare R.N.* // J. Phys. Chem. – 1996. – **100**. – P. 7938.
6. *Orr-Ewing A.J., Simpson W.R., Rakitzis T.P., Kandel S.A., Zare R.N.* // J. Chem. Phys. – 1997. – **106**. – P. 5961.
7. *Rakitzis T.P., Kandel S.A., Lev-On T., Zare R.N.* // J. Chem. Phys. – 1997. – **107**. – P. 9392.
8. *Kandel S.A., Zare R.N.* // J. Chem. Phys. – 1998. – **109**. – P. 9719.
9. *Bechtel H.A., Camden J.P., Brown D.J.A., Zare R.N.* // J. Chem. Phys. – 2004. – **120**. – P. 5096.
10. *Kim Z.H., Bechtel H.A., Camden J.P., Zare R.N.* // J. Chem. Phys. – 2005. – **122**. – P. 082303.
11. *Zhang B., Liu K.* // J. Chem. Phys. – 2005. – **122**. – P. 101102.
12. *Chao S.D., Skodje R.T.* // J. Chem. Phys. – 2003. – **119**. – P. 1462; Theor. Chem. Acc. – 2002. – **108**. – P. 273.
13. *El-Din Kamal M.T., El-Wallid Sedik S., Talaat H.* // Z. Phys. Chem. – 2008. – **222**. – P. 1693–1701.
14. *Castillo A., Bañares J.* // Chem. Phys. – 2006. – **125**. – P. 124316.
15. *Corchado J.C., Truhlar D.G., Espinosa-García J.* // J. Chem. Phys. – 2000. – **112**. – P. 9375.
16. *Martínez R., González M., Defazio P., Petrongolo C.* // J. Chem. Phys. – 2007. – **127**. – P. 104302.
17. *Sansón J., Corchado J.C., Rangel C., Espinosa-García J.* // J. Chem. Phys. – 2006. – **124**. – P. 074312.
18. *Defazio P., Petrongolo C.* // J. Chem. Phys. – 2006. – **125**. – P. 064308.